REPORT DOCUMENTATION PAGE

Form Approved OMB NO. 0704-0188

1. REPORT DATE (DD-MM-YYYY)	2. REPORT TYPE	3. DATES COVERED (From - To)
14-02-2016	Final Report	1-Sep-2012 - 31-Aug-2015

4. TITLE AND SUBTITLE
Development of the III--V Barrier PhotoDetectorHeterostructures for Spectral Range Above 10 μm

5a. CONTRACT NUMBER
W911NF-12-2-0057

5b. GRANT NUMBER

5c. PROGRAM ELEMENT NUMBER
611102

6. AUTHORS
Gregory Belenky, Dmitri Donetski, Leon Shterengas, Sergey Suchalkin, Gela Kipshidze, Youxi Lin

5d. PROJECT NUMBER

5e. TASK NUMBER

5f. WORK UNIT NUMBER

7. PERFORMING ORGANIZATION NAMES AND ADDRESSES
Research Foundation of SUNY at Stony Brc
W-5510 Melville Library

Stony Brook, NY 11794 -3362

8. PERFORMING ORGANIZATION REPORT NUMBER

9. SPONSORING/MONITORING AGENCY NAME(S) AND ADDRESS (ES)
U.S. Army Research Office
P.O. Box 12211
Research Triangle Park, NC 27709-2211

10. SPONSOR/MONITOR'S ACRONYM(S)
ARO

11. SPONSOR/MONITOR'S REPORT NUMBER(S)
62447-EL.21

12. DISTRIBUTION AVAILIBILITY STATEMENT
Approved for Public Release; Distribution Unlimited

13. SUPPLEMENTARY NOTES
The views, opinions and/or findings contained in this report are those of the author(s) and should not contrued as an official Department of the Army position, policy or decision, unless so designated by other documentation.

14. ABSTRACT
Novel approach to growth of quality narrow gap InAsSb-based materials using metamorphic buffers on GaSb substrates was pursued. The developed GaInSb and AlInSb graded buffers served as a platform for growth of strain-free low-dislocation-density bulk InAsSb layers. The ability to select the lattice constant up to 3 % greater than that of GaSb eliminated the lattice constant design constrain in the realization of III-V narrow gap semiconductors grown pseudomorphically on the available substrates. The buffers were developed for InAsSb alloys with Sb compositions in the range from 20 to 65 %. The bulk InAsSb layers showed the energy gaps as low

15. SUBJECT TERMS
Metamorphic growth, MBE, LWIR, InAsSb, carrier lifetime, barrier photodetectors

16. SECURITY CLASSIFICATION OF:			17. LIMITATION OF ABSTRACT	15. NUMBER OF PAGES	19a. NAME OF RESPONSIBLE PERSON
a. REPORT	b. ABSTRACT	c. THIS PAGE			Gregory Belenky
UU	UU	UU	UU		19b. TELEPHONE NUMBER: 631-632-8397

RPPR

as of 21-Sep-2018

Agency Code:

Proposal Number: **Agreement Number:**

Organization:
Address: , ,
Country:
DUNS Number: EIN:
Report Date: Date Received:
for Period Beginning and Ending
Title:
Begin Performance Period: **End Performance Period:**
Report Term: -
Submitted By: Email:
Phone:

Distribution Statement: -

STEM Degrees: **STEM Participants:**

Major Goals:

Accomplishments:

Training Opportunities:

Results Dissemination:

Plans Next Period:

Honors and Awards:

Protocol Activity Status:

Technology Transfer:

Development of the III-V Barrier Photo Detector Heterostructures for Spectral Range Above 10 μm

Final Progress Report

Principal Investigator: Prof. Gregory Belenky

Table of contents:

1. List of illustrations

Figure 1. Reciprocal Space Map (RSM) for assessment of the buffer grade relaxation, determination of the lateral lattice constant on top of the buffer and residual strain in a bulk InAsSb layer. The asymmetric (335) RSM for structure $InAsSb_{0.44}$ for the azimuthal angles of 0 (left) and 180 degrees (right) allowed to average the contribution of a tilt in the relaxed part of the buffer to the result of lattice constant measurements [1]. A nearly 100 % relaxed part of the buffer follows the solid (red) line. The dashed (vertical) lines denote the top strained part of the buffer with the lateral lattice constant $a_{||} \approx 3\sqrt{2}/0.68 = 6.22$ A. The red reflex point marked with L corresponds to a low residual strain InAsSb layer with the lattice constant similar to that of the top of the buffer.

Figure 2.Crosssectional Transmission Electron Microscopy (XTEM) image for assessment of the thickness of the top dislocation-free buffer section, virtual substrate and dislocation gliding. XTEM image (220 bright field with two beam condition) of the metamorphic structure with 0.5-μm thick $InAs_{0.8}Sb_{0.2}$ bulk layer grown on GaInSb graded buffer [2] shows that the dislocations are confined within the bottom relaxed part of the buffer.

Figure 3. The dependence of photoluminescence (PL) maxima on Sb composition (a) and the PL spectra (b) measured at T =77 K. With accounting for thermal broadening the lowest energy gap for the bull InAsSb was estimated to be 90 meV.

Figure 4. The bulk InAsSb barrier heterostructure cross-section (a). Arrows show lateral diffusion of minority carriers; Minority hole lifetime, diffusion length and hole mobility were determined from the transient response of barrier structures to a pulsed excitation (b). F denotes a fast response, a non-exponential slow response fits with a 165 ns carrier lifetime and a 9 μm diffusion length [8].

Figure 5. Quantum efficiency spectra (a) and temperature dependence of dark current (b) in heterostructures consisting of bulk InAsSb absorber and AlInAsSb barrier for assessment of the material absorption, efficiency of hole transport and presence of depletion region at the heterointerface with absorber.

Figure 6. Photoluminescence (a) and photoconductivity (b) spectra in short –period $InAsSb_x$ /$InAsSb_y$ Strained-Layer Superlattices (SLS) in the wavelength range up to 20 μm [12].

2. Subject of the research and the problem solved

Novel approach to growth of quality narrow gap InAsSb alloys for wavelength range from 5 to 12 μm using metamorphic buffers on GaSb substrates was pursued. The developed GaInSb and AlInSb buffers served as a platform for strain-free low-dislocation-density bulk InAsSb layers. **The ability to select the lattice constant up to 3 % greater than that of GaSb eliminated the lattice constant design constrain in the realization of III-V narrow gap semiconductors** grown pseudomorphically on GaSb or other binary substrates. The developed quality bulk InAsSb layers with energy gaps as low as 90 meV at 77 K exhibit strong fundamental absorption and long diffusion length of minority holes. The effort was focused on determination of the fundamental parameters of InAsSb alloys with target Sb compositions covering the range from 20 to 65 %. The solved challenges include selection of the buffer grade composition rate and growth temperature for gliding dislocations in the buffer away from the growth direction, determination of the lateral lattice constant of the top strained layer of the buffer, selection of the growth regime for InAsSb alloys to obtain large Sb compositions in the alloys. There were challenges to solve in material characterization including measurements of the background concentrations and minority carrier lifetimes. There was a challenge to select barrier composition in barrier heterostructures for the minimal valence band offset at the interface of InAsSb and AlInAsSb layers necessary for the efficient minority hole transport. The developed InAsSb-based detector heterostructures demonstrate high quantum efficiency consistent with the absorption spectrum and efficient hole transport of bulk layers as well as long carrier lifetime of Ga-free materials.

3. Summary of the most important results

1. **The principles of growth of strain-free, low-dislocation-density bulk InAsSb layers with energy gaps in the range of 0.1-0.2 eV on linearly graded GaInSb and AlInSb metamorphic buffers were confirmed with Reciprocal Space Mapping (RSM), Transmission Electron Microscopy (TEM) imaging and electron diffraction characterization methods on a statistically sufficient set of samples grown in both Stony Brook University and Army Research Laboratory.** The lattice parameters of the individual layers in the metamorphic heterostructures were quantified using RSM measured near the asymmetric (335) reflex of the GaSb substrate (Figure 1). The RSM measurements were performed at 0 and 180 azimuthal angles with respect to the [110] direction. The [110]

and [-1-10] RSM data were averaged to compensate for a tilt of the metamorphic layers with respect to GaSb substrate plane. A strong reflex from InAsSb layer marked with L in Figure 1 situated on solid red line corresponding to completely relaxed crystal proved that InAsSb layers had undistorted cubic crystals (unstrained) with the lattice constant of a = 5/0.8 = 6.25 A. That lattice constant corresponds to Sb composition of 44 %. The top part of the compositionally graded buffer follows the vertical (dashed) line confirming pseudomorphic growth of the top of the buffer with a residual strain.

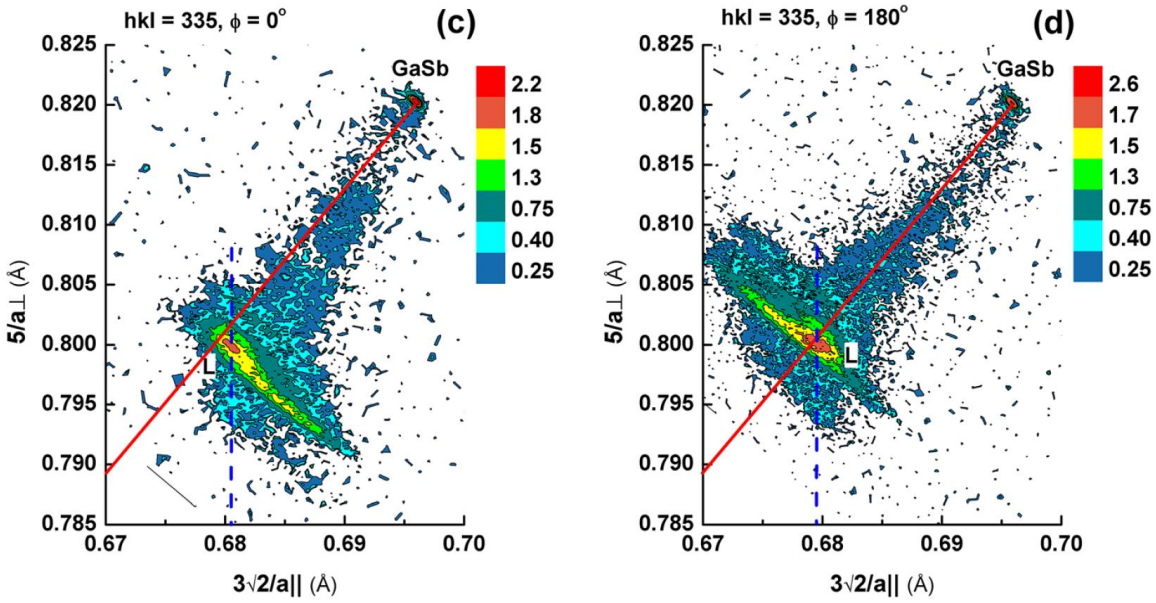

(a) (b)

Figure 1. Reciprocal Space Map for assessment of the buffer grade relaxation, determination of the lateral lattice constant on top of the buffer and residual strain in a bulk InAsSb layer. Asymmetric (335) Reciprocal Space Maps (RSM) for structure $InAsSb_{0.44}$ for the azimuthal angles of 0 (a) and 180 degrees (b) for averaging the contribution of a tilt in the relaxed part of the buffer to the result of lattice constant measurements [1]. A nearly 100 % relaxed part of the buffer follows the solid (red) line. The dashed (vertical) lines denote the top strained part of the buffer with the lateral lattice constant $a_{||} \approx 3\sqrt{2}/0.68 = 6.22$ A. The red reflex point marked with L corresponds to a low residual strain InAsSb layer with the lattice constant similar to that of the top of the buffer.

It was concluded that InAsSb layer was grown pseudomorphically on the top of the buffer layer with a residual in-plane strain to be below 0.1 %. The amount of residual strain in the heterostructure was determined by direct measurement of the in-plane (100) and (010) and perpendicular (001) lattice parameters from the RSM data. Low residual strain values imply no

relaxation and thus no formation of misfit dislocations in InAsSb layers. The latter was confirmed by TEM data (Figure 2). A correlation between the length of the top dislocation free region and the buffer composition grading rate and residual strain was observed in accordance with theoretical expectations.

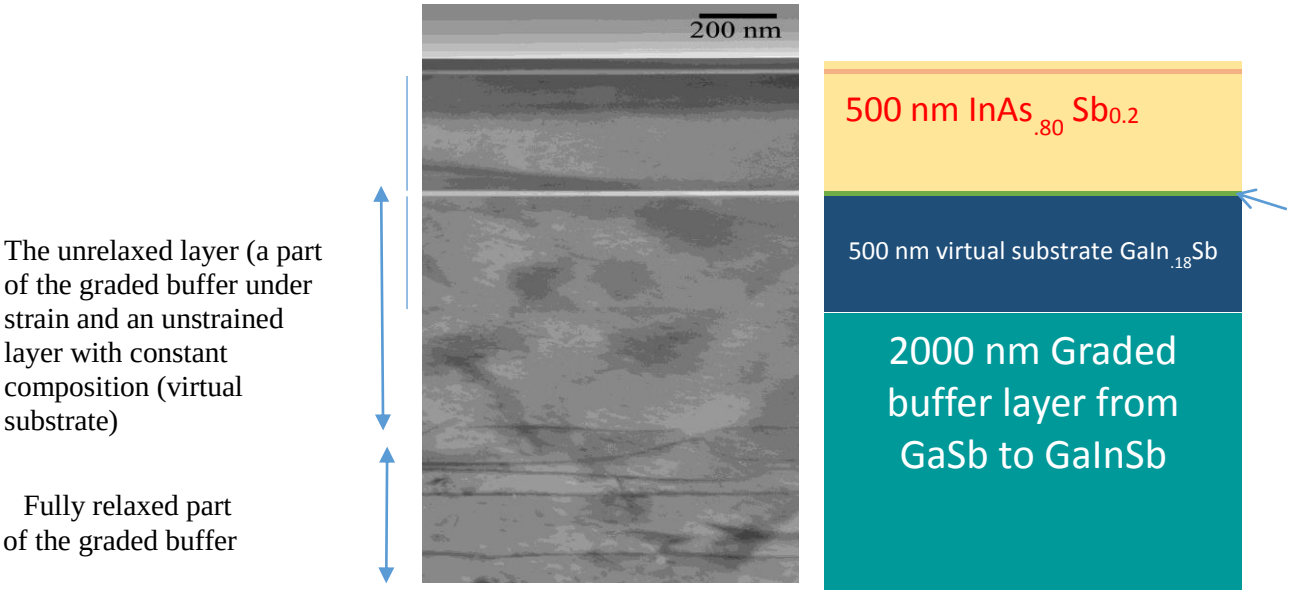

Figure 2.Crosssectional Transmission Electron Microscopy (XTEM) image for assessment of the thickness of the top dislocation-free buffer section, virtual substrate and dislocation gliding. XTEM image (220 bright field with two beam condition) of the metamorphic structure with 0.5-µm thick $InAs_{0.8}Sb_{0.2}$ bulk layer grown on GaInSb graded buffer [2] shows that the dislocations are confined within the bottom relaxed part of the buffer.

2. **The lowest energy gap of InAsSb alloys with large Sb compositions (55 -65 %) was determined to be 90 meV at T = 77 K.** The PL spectra were measured for a large group of samples with various Sb compositions in InAsSb layer which required various buffer design parameters, respectively. The compiled dependence of the PL maximum versus Sb composition in InAsSb is shown in Figure 3a [2].

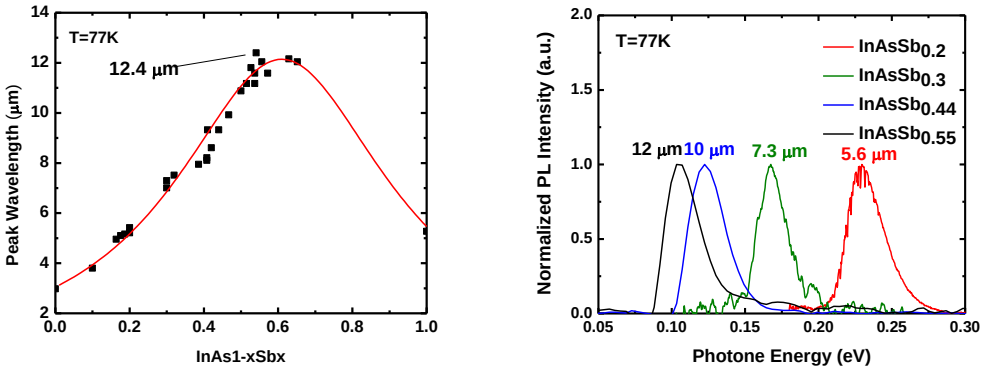

(a) (b)

Figure 3. The dependence of PL maximum on Sb composition (a) and the PL spectra (b) at T =77 K. With accounting for thermal broadening the lowest energy gap for the bull InAsSb is estimated to be 90 meV.

3. Figure 3b shows the actual PL spectra for the alloys with various Sb compositions measured at T = 77 K. These spectra demonstrate thermal broadening which has to be taken into account in estimation of the energy gap of the materials. It was done by subtracting 2 k_BT /e =13 meV from the energy of the PL maxima. The typical full-width at half-maximum (FWHM) of PL spectra at T =20 K was 14 meV which indicated high crystalline quality of the materials.

4. **Carrier recombination properties of Ga-free narrow gap materials have been studied by measuring minority carrier lifetime in heterostructures with unintentionally doped, n-doped and p-doped absorbers in a range of excess carrier concentrations.** Three approaches to measurement of carrier lifetime have been developed aimed at obtaining reliable data under lowest possible excess carrier concentration: (1) time–resolved photoluminescence (TRPL) measurements with transient response to a pulsed excitation [4], (2) TRPL with optical response to small amplitude sinwave-modulated excitations also referred to as optical modulation response (OMR) [4] and (3) transient response of photocurrent in barrier heterostructures due to lateral diffusion of minority carriers [7-8].

In undoped InAsSb alloys with 40 % Sb composition grown on metamorphic buffers the minority hole lifetime up to 185 ns at T = 77 K was measured [7].

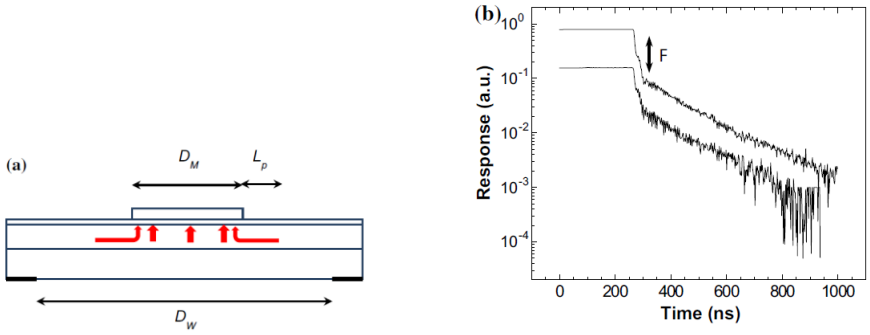

Figure 4. The bulk InAsSb barrier heterostructure cross-section (a). Arrows show lateral diffusion of minority carriers; Minority hole lifetime, diffusion length and hole mobility were determined from the transient response of barrier structures to a pulsed excitation (b). F denotes a fast response, a non-exponential slow response fits with a 165 ns carrier lifetime and a 9 μm diffusion length [8].

The difference in the decay times (a fast part of the response denoted by F in Figure 4b followed by a slow part was used to separate the vertical and lateral components of the response in time domain. This innovative approach showed that under the pulsed excitation the waveform of the decay for the lateral (slow) signal is defined by the carrier lifetime and the diffusion length. The electric field was estimated and it was shown that one can neglect the effect of hole drift on the response decay at least for the carrier transport in the lateral direction. The hole carrier lifetime of 165 ns and the diffusion time of 9 μm were obtained from fitting of the non-exponential decay to the analytically-obtained expression. **The excess hole concentration in lifetime measurements was estimated to be of 5x10^{13} 1/cm^3 level.** Such a low excess carrier concentration was found to be critical for adequate minority carrier lifetime measurements as the background electron concentration is typically in a range of low 10 ^{15} cm^{-3}. Using these data the hole mobility was calculated to be of 1000 cm^2/Vs at T =77 K. The vertical transition time for diffusion of holes across a 1-micron-thick absorber of 2 ns was confirmed by the measurement of the frequency response for a 100-μm-side square-contact mesa structure.

The minority hole lifetime of a 200 ns level in bulk InAsSb grown metamorphically is comparable to the hole lifetime of 400 ns in Ga-free strained layer superlattices (SLS) with similar energy gaps grown pseudomorphically on GaSb [4]. The probability of the optical transitions in those SLS was estimated to be lower by a factor of 2-3 compared to bulk InAsSb alloys. The latter is due to wide InAs wells for electrons resulting in strong confinement of holes in InAsSb wells in InAsSb/InAs SLS grown lattice-matched to GaSb. The hole

confinement in turn implied a reduced overlap of the electron and hole wavefunctions hence weaker recombination processes and longer lifetimes in a presudomorphically grown InAs/InAsSb SLS compared to that in bulk InAsSb alloys. Thus, with accounting for strong e-h overlap in bulk InAsSb alloys one can conclude about high quality of bulk InAsSb alloys grown on the metamorphic buffers.

A slow part of the response decay in bulk InAsSb barrier heterostructures allows for **determination of the diffusion length and mobility for minority holes, respectively, found to be 9 μm and 1000 cm^2/Vs, respectively, at T =77 K** [7]. The fast response time of 2 ns confirmed the calculated mobility of minority holes. The expression below was used for fitting the slow part of responses.

$$S \propto \exp\left(-\frac{t}{\tau_p}\right)\mathrm{Erf}\left(\frac{D_W - D_M}{4}\sqrt{\frac{\tau_p}{L_p^2 t}}\right)$$

Here Erf is Error function with argument including dimensions of mesa D_M, and window D_W in the contact, in Figure 4a, τ_p and L_p are hole lifetime and diffusion length, respectively. The above expression was derived as a part of the project effort.

5. The background carrier concentration and electron mobility were measured in bulk InAsSb layers using the mobility spectrum approach in samples with the narrow gap layer thickness varied by etching. This approach allowed to separate the contributions of the heterointerface and surface conductivity channels into the Hall effect results. **In unintentionally-doped InAsSb with Sb composition near 40 % the electron concentration and mobility at T =77 K were found to be 2.5 x10^{15} cm^{-3} and 140,000 cm^2/Vs**, respectively [9].
6. Using the transient response of photocurrent in barrier heterostructures the minority hole lifetime was measured in bulk InAsSb doped with Tellurium to the electron concentrations of 2, 4 and 7 x10 ^{16} cm^{-3}. The measured minority hole lifetime values were 185, 100 and 80 ns at T =77 K. The electron concentration values were determined using the effective mass and the Fermi level energies. The latter energies were estimated from the quantum efficiency spectra. These data suggest an estimate of **200 ns of Auger-limited carrier lifetime in n=7x10^{16} cm^{-3} InAsSb with Sb =40% at T=77 K**. Extrapolation of the data to the background concentration of 10^{15} cm^{-3} level would result in Auger lifetime of a microsecond

scale. Thus, the minority hole lifetime in order of 200 ns measured in unintentionally doped InAsSb at T = 77 K was limited by Shockley-Read-Hall (SRH) recombination processes.

7. **The electron effective masses of InAsSb alloys with 40 and 63 % Sb were found to be 0.011 and 0.0065 of free electron mass** from cyclotron resonance (CR) spectra [10]. These data allowed to estimate the concentration of electrons in Te-doped InAsSb alloys.
8. Due to superior electron mobility, photodetectors with p-doped absorbers can operate at elevated temperatures and with faster response compared to those in detectors with n-type absorbers. It was important to determine the dependence of the electron lifetime on p-doping level. **The minority electron lifetime was measured in Be-doped InAs/InAsSb SLS with hole concentrations of $6x10^{16}$ and $3x10^{17}$ cm^{-3}** determined from Hall data and confirmed by transition point from linear to quadratic recombination with change of the slope of the dependence of peak PL intensity on pulse excitation energy [4]. **For the above doping levels the minority electron lifetime values were determined to be 45 and 8 ns, respectively.** Considering the superior electron mobility, a 45 ns electron lifetime at T = 77 K could be sufficient for adequate quantum efficiency of photodetectors with Ga-free absorbers doped with Be to free hole concentration levels of mid 10^{16} cm^{-3}.
9. **The graded GaInSb metamorphic buffer recipes have been developed for the bulk InAsSb layers with Sb compositions of 50 and 65 %. An increase of the PL wavelength to about 11 μm was observed for the InAsSb with the 50 % of Sb composition.**
10. **Growth of the barrier heterostructures with a 50 % Sb composition in InAsSb absorber with the thickness up to 3 μm and a lattice-matched AlInSb barrier was demonstrated.** The quantum efficiency (QE) spectra started from the wavelength of 11 μm. For the structures with the absorber thicknesses of 1, 2 and 3 μm the QE at 8 μm wavelength were measured to be of 22, 29 and 39 %, respectively. It was found important to determine the position of the top of the valence band and the valence band offset at the absorber-barrier interface for reduction of the required bias voltage, the dark current, and its dependence on bias and temperature.
11. An evidence of the bowing of the valence band of InAsSb alloys was determined by an innovative approach from pulsed excitation spectra of InAs/InAsSb SLS. **The data suggest the valence band bowing parameter of -0.3 eV** [3]. These data are important for selection of the composition of the alloy of the barrier heterostructures with minimal valance band

offset for efficient minority hole transport across the barrier with low external bias/ low dark current.

12. For study of physical phenomena contributing to the dark current the design of barrier heterostructures was optimized with acceptance of **undoped AlInAsSb barriers with the As composition of 10 %** lattice matched to the bulk InAsSb with 40 % Sb composition. (Figure 5a.) [5- 8]

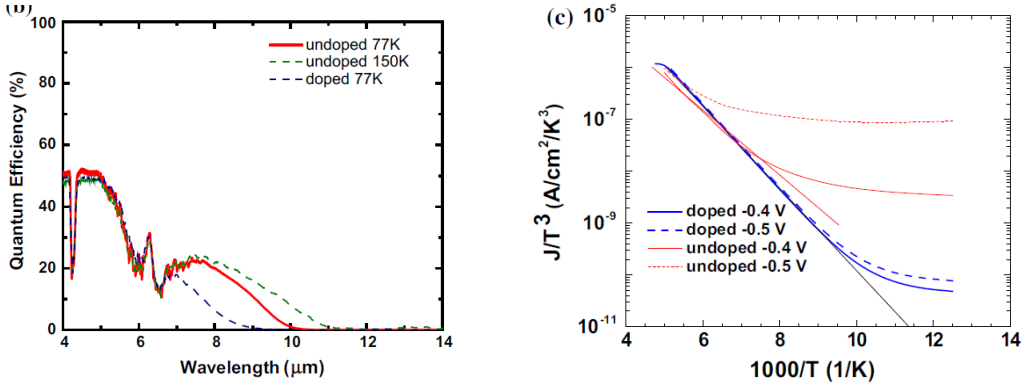

(a) (b)

Figure 5. Quantum Efficiency spectra (a) and temperature dependences of the dark current (b) versus for two bias voltage for InAsSb/ALInAsSb barrier hetertostructures with undoped and lightly doped (n~10^{16} cm^{-3}) absorbers. Reduction of the dark current with doping was attributed to decrease of the depleted part of the absorber at the interface with the barrier.

The heterostructures of new design with undoped barriers showed the saturation of the quantum efficiency at the bias of 0.4 V compared to 0.9 V for the devices of the previous generation with the ternary AlInSb barriers. The I-V characteristics in semilog scale were less dependent on bias voltage in the range where QE saturates with bias (Figure 5b). The improvements in newly developed barrier heterosructures were attributed to reduction of the valence band offset at the heterointerface. The reduction of the dark current component with light doping of the absorber (n~10^{16} cm^{-3}) was attributed to reduction of the width of the depletion region at the interface with the barrier. The barrier structures with 1 μm thick absorbers showed the QE starting from the wavelength of 10 μm. The wavelength of 8 μm was selected as the reference point for comparison. For the detectors with a 1-μm-thick absorbers and 40 % Sb composition the QE at 8 μm of 18 % was measured. This is a

significant improvement over a 10 % QE value reported earlier for the devices with the ternary AlInSb barriers doped with Be to the level of $1x10^{16}$ $1/cm^3$.

13. **The fundamental absorption spectrum of InAsSb with 40 % Sb composition was determined directly from the transparency spectra of the epilayer and the substrate.** The absorption coefficient value and its spectral behavior were found to be similar to that reported in the literature for HgCdTe with similar energy gap. The Urbach tail parameter W was found to be consistently small (W < 5 meV). **We find that one of the reasons for such an abrupt absorption edge and its small broadening in ternary alloys with random distribution of elements is a nearly constant energy gap of InAsSb alloys in the range of large Sb compositions close the energy gap minimum. This feature of narrow gap InAsSb alloys means a good uniformity of energy gap useful for infrared sensing and imaging technology in a long wave infrared (LWIR) region.**
14. The dependences of the dark current on bias voltage were measured in the temperature range of T = 77- 200 K. The dependence of the QE on the bias voltage reaches a nearly maximum value at V = -0.4 V. A continuing increase of the QE after the bias voltage of -0.4 V suggests that a residual barrier for minority hole transport is not completely suppressed at this bias. Further optimizations of both the barrier composition and doping would be desirable for elimination of the valence band discontinuity between the absorber and the barrier layers for reduction of the required bias voltage and for elimination of the voltage dependence of the dark current. Thus, one can conclude that the current transport is not completely diffusion limited. Still, comparing the temperature dependences of the dark current in the heterostructures with intentionally doped absorbers at V1 = -0.4 V and V2 = -0.5 V one can see that the difference between the dark current values becomes small at elevated temperatures, starting from as low as T =110 K. It suggests that **hole transport is nearly diffusion limited at elevated temperatures above T =110 K**. Note that detector at T =77 K exposed to thermal background radiation from a room temperature object would have photocurrent at least an order of magnitude greater than the dark current value at that temperature.
15. Characterization of AlInAsSb alloys with various Al compositions grown on metamorphic buffers with the top lattice constant equal to that of InAsSb for LWIR range was performed. The AlInAsSb alloys were intended for use as a mid-wave infrared absorber in bi-color

devices. Alternatively these alloys can be used as barriers for LWIR InAsSb absorbers. The dependence of the energy gap on Al composition was determined [11].

16. The energy gap of III-V semiconductor compound materials can be further reduced with short-period modulation of Sb composition resulting a short-period SLS. The efficient hole transport was preserved due to anticipated tunneling of hole in the vertical direction and presence of a sufficiently wide hole miniband. Figure 6 shows the preliminary data for the PL spectra (a) and photoconductivity spectra (b) in barrier heterostructures with absorbers consisting of InAsSb with modulated Sb composition (short –period $InAsSb_x/InAsSb_y$ SLS).

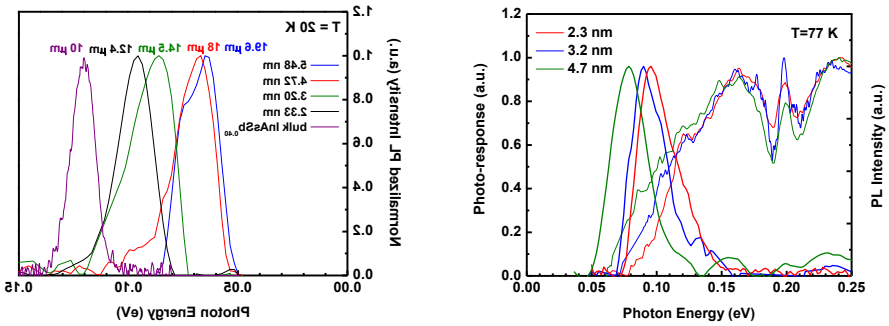

Figure 6. Photoluminescence (a) and photoconductivity (b) spectra in short –period $InAsSb_x$ /$InAsSb_y$ Strained-Layer Superlattices (SLS) in the wavelength range up to 20 μm [12].

Summarizing the effort on study of fundamental properties of bulk InAsSb alloys, no limitations on the performance of the devices with bulk InAsSb absorbers were found. The devices with an undoped absorbers of n-type showed no surface current. The SRH hole lifetime of a 200 ns level can be increased with material growth optimization, use of a new MBE chamber with a lower background impurity levels solely dedicated to growth of detector heterostructures. The absorption coefficient, the effective electron mass at the bottom of the conduction band were found to be similar to that for HgCdTe with similar energy gaps. Further research effort is required to determine Auger recombination coefficients while the available lifetime data look optimistic. The bulk materials exhibit a low temperature energy gap as low as 90 meV. The feasibility of extension of the absorption edge of InAsSb-based materials grown on metamorphic buffers up to a 20 μm

wavelength and beyond was demonstrated suing short-period InAsSb-based SLS with modulated Sb composition in adjacent layers of a SLS cell.

4. Bibliography (Publications)

Book chapters and Peer-reviewed Journals

1. D. Wang, D. Donetsky, Y. Lin, G. Kipshidze, L. Shterengas, G. Belenky, W. L. Sarney, S. P. Svensson,. InAs1-xSbx alloys with native lattice parameters grown on compositionally graded buffers: structural and optical properties, Singapore: World Scientific Publishing Corp., 2013.
2. G. Belenky. D. Wang, Y. Lin, D. Donetsky, G. Kipshidze, L. Shterengas, D. Westerfeld, W. L. Sarney, S. P. Svensson, Metamorphic InAsSb/AlInAsSb heterostructures for optoelectronic applications, *Appl. Phys. Lett.*, **102**, 111108 (2013).
3. Y. Lin, D. Wang, D. Donetsky, L. Shterengas, G. Kipshidze, G. Belenky, S. P. Svensson, W. L. Sarney, H. S. Hier. Conduction- and Valence-Band Energies in Bulk InAs1-x Sb x and Type II InAs1-x Sb x /InAs Strained-Layer Superlattices, *J. of Electron. Mater.*, **42**, 918 (2013).
4. Y. Lin, D. Wang, D. Donetsky, G. Belenky, H. Hier, W. L. Sarney, S. P. Svensson. Minority Carrier Lifetime in Beryllium-Doped InAs/InAsSb Strained Layer Superlattices, *J. of Electron. Mater.*, **43**, 3184 (2014).
5. D. Wang, D. Donetsky, G. Kipshidze, Y. Lin, L. Shterengas, G. Belenky, W. Sarney, S. P. Svensson. Metamorphic InAsSb-based barrier photodetectors for the long wave infrared region, *Appl. Phys. Lett.*, **103**, 051120 (2013).
6. Y. Lin, D. Wang, D. Donetsky, G. Kipshidze, L. Shterengas, G. Belenky, W. L Sarney, S. P. Svensson. Structural and Optical Characteristics of Metamorphic Bulk InAsSb, *Intern. J. of High Speed Electronics and Systems*, 1450021 (2014).
7. Y. Lin, D. Wang, D. Donetsky, G. Kipshidze, L. Shterengas, L. E. Vorobjev, G. Belenky, Transport properties of holes in bulk InAsSb andperformance of barrier long-wavelength infrared detectors, *Semicond. Sci. and Technol.*, **29**, 112002 (2014).
8. Y. Lin, D. Donetsky, D. Wang, D. Westerfeld, G. Kipshidze, L. Shterengas, W. L. Sarney, S. P. Svensson, G. Belenky, Development of Bulk InAsSb Alloys and Barrier Heterostructures for Long-Wave Infrared Detectors, *J. of Electron. Mater.*, **44,** 3360, (2015):
9. S. P. Svensson, F. J. Crowne, H .S. Hier, W L Sarney, W. A. Beck, Y. Lin, D. Donetsky, S. Suchalkin, G. Belenky. Background and interface electron populations in InAs0.58Sb0.42, *Semicond. Sci. and Technol.*, **30** (3), 035018 (2015).
10. S. Suchalkin, J. Ludwig, G. Belenky, D. Smirnov, B. Laikhtman, S. Luryi, W.L. Sarney, G. Kipshidze, S.P. Svensson, Y. Lin, L.Shterengas, Electronic properties of unstrained unrelaxed narrow gap InAsxSb1-x alloys, *J. of Physics D: Applied Physics*, **49** (10), 105101 (2016).

11. W. L. Sarney, S. P. Svensson, D. Wang, D. Donetsky, G. Kipshidze, L. Shterengas, Y. Lin, G. Belenky. AlInAsSb for MLWIR detectors, *J. of Cryst. Growth*, **425**, 357 (2015):
12. G. Belenky, Y. Lin, L. Shterengas, D. Donetsky, G. Kipshidze and S. Suchalkin, Lattice parameter engineering for III–V long wave infrared photonics, *El. Lett.*, **51** (19) 1521 (2015).

Papers in Conference Proceedings

1. D. Wang, Y. Lin, D. Donetsky, G. Kipshidze, L. Shterengas, G. Belenky, S. P. Svensson, W. L. Sarney, H. Hier. Infrared Emitters and photodetectors with InAsSb bulk active region, SPIE Defense, Security+ Sensing, *Proc. SPIE*, **8704**, 870410-1 (2013).

Conference presentations not published in Proceedings

1. "Metamorphic antimonides for infrared photonics", presented by L.Shterengas on the Workshop in Army Research Laboratory, June 18, 2013.

2. "Development of infrared photodetectors with bulk InAsSb absorbers", presented by D. Donetski on the Workshop in Army Research Laboratory, June 18, 2013.

3.. Development of bulk (Al)InAsSb alloys and InAsSb/AlInAsSb heterostructures for L/MWIR applications, D. Donetsky, S. P. Svensson, W. L. Sarney, H. S. Hier, D. Wang, G. Kipshidze, L. Shterengas, Y. Lin, G. Belenky, SPIE Photonics West, San Francisco, CA, February 4, 2014

4. Progress in development of LWIR detectors with bulk InAsSb absorbers, SPIE Photonics West, San Francisco, February 8, 2015

5. Fundamental absorption and recombination properties of bulk InAsSb with 40 % Sb and comparison with HgCdTe Rule 07, Stony Brook-ARL meeting, Stony Brook, July 14, 2015.

Ongoing research and anticipated manuscripts

1. Fundamental absorption in bulk InAsSb and short-period InAsSb SLS.
2. Auger lifetime in bulk InAsSb.
3. Ordering in InAsSb SLS.